

Leech-Inspired Shape-Encodable Liquid Metal Robots for Reconfigurable Circuit Welding and Transient Electronics

Ben Wang¹, Baofeng Zhang¹, Yongzhu Tan¹, Fengtong Ji², Guanghui Lv¹, Chengfeng Pan², Stephan Handschuh-Wang¹, Li Zhang², and Xuechang Zhou¹

¹Shenzhen University

²The Chinese University of Hong Kong

May 4, 2022

Abstract

Deformability and self-adaptability are important for soft robots in order to deal with uncertain and varying situations and environments during movement and navigation. Droplet-based robots are great candidates to travel inside narrow and constrained spaces without damaging the interfaces due to their extreme deformability and liquid nature, which enables smooth contact between robots and target spaces. Here, we propose magnetic liquid metal droplet robots, comprising liquid metal and carbonyl iron, that can perform reversible telescopic deformation, bending, and on-demand locomotion. The magnetic liquid metal-based robots can perform on demand and reversible coalescence and splitting by intricately applying magnetic fields. Importantly, the liquid metal robot can perform phase transition to fix the desired shape after the programmable shape encoding. The liquid metal-based soft robots can serve as dynamic and recyclable switches for complex circuits, and are capable of repairing damaged sections of microcircuits by remote actuation, controllable coalescence, and on-demand circuit welding. The technology provides a new application scenario of droplet-based soft robots for on-demand circuit welding and transient recyclable electronics.

Corresponding author(s) Email: X.Z.: xczhou@szu.edu.cn; L.Z.: lizhang@mae.cuhk.edu.hk; B.W.: benwang@szu.edu.cn

ToC Figure

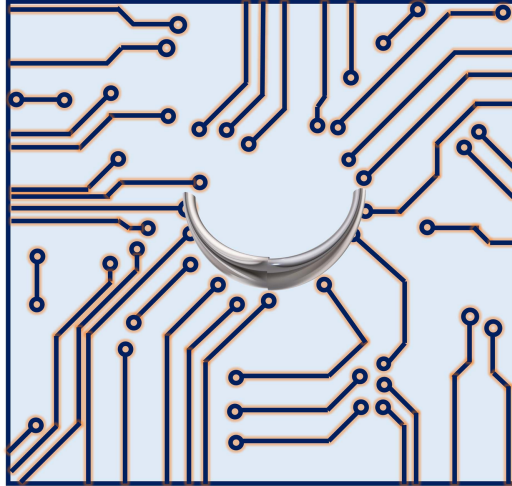


Figure 1: **ToC Figure.** Liquid metal-based soft robots serve as dynamic and recyclable switches for complex circuits, and are capable of repairing damaged sections of microcircuits by remote actuation, controllable coalescence, and on-demand welding.

1. Introduction

Robotics and especially, soft robotics, a sub-branch of robotics, have recently attracted broad interest in the scientific community.^[1,2] This interest is fueled by the flexible and deformable nature of the materials used, and (for some) that they can be deformed upon a specific trigger, i.e., temperature, pH, magnetic field, and electric field, and thus, feature distinct advantages for their application in cargo transportation, drug delivery, microsurgery and so forth.^[3-6] For example, soft robots have been introduced, which can navigate and pass-through narrow gaps that are smaller in size than the initial robot shape via (triggered) deformation (triggered shape transformation).^[7-12] In addition, the suppleness of the soft robots can mitigate damage to an object or body in contact with the robot.

Evolution and adaption to everchanging environments have brought about a large variety of soft-bodied living things, which offer abundant inspiration to the design and construction of soft robotics.^[13] For instance, mollusks (invertebrates) can stretch, curl up, and travel by relying on a complex mixture of biophysical and chemical signals originating from the surrounding (environmentally triggered transformations). For example, leeches, which belong to the phylum mollusks, can perform multimodal movements, including reconfigurable deformation, swimming, inchworm-like movement, and peristalsis, according to different environmental triggers, i.e., temperature and chemical composition of the water.^[14] Inspired by the phylum mollusk, various soft robots have been developed, that can perform reconfigurable and self-adaptable actuation in different environments.^[15-18] Therein, droplet-based soft robots have attracted great attention due to their excellent mechanical properties stemming from their liquid nature, including the high softness and extreme deformability.^[19] Plenty of droplet-based soft robots have been developed in recent years, such as water droplet robots,^[20-23] ferrofluid droplet robots,^[24,25] oil droplet robots,^[26] and liquid metal droplet robots^[27-35] for a variety of engineering and biomedical applications, such as drug delivery, cargo transportation, and mixing of chemicals in lab-on-a-chip applications.^[24,32,36,37] Furthermore, fundamental studies on droplet-based soft robots have provided striking insights into the physics and hydrodynamics of droplets spanning a wide range of spatial scale (macro to microscale).^[38,39] Although the deformability and mobility of the droplet-based robots have been advantageous for ample applications, most of the droplet-based robots offer only low electrical conductivity, limiting their range of applications substantially.

In this regard, room temperature liquid metals, metals and alloys that are in the liquid state at or near room

temperature, have garnered extensive attention from the scientific community as well as industry due to their extraordinary combination of physical properties.^[40-44] Several metals and alloys are known and in use for experiments and industrial applications. Broadly known are alloys based on Bi, such as the ternary alloy Field's metal and quaternary alloy Wood's metal, Pb-based alloys, and gallium and its alloys. Especially, the Ga-based liquid metals, that are gallium, the eutectic mixture of Ga and In (EGaIn), the eutectic mixture of Ga, In and Sn at a composition of Ga 68.5 wt%, In 21.5 wt%, Sn 10 wt% (Galinstan), and the Ga-Sn mixture have been investigated due to the low melting point and strong supercooling.^[44-48] Furthermore, the gallium-based liquid metals feature (values for Galinstan) high electrical ($0.34 \cdot 10^5$ S/cm) and thermal conductivity ($[?] 25$ W/m²K), high surface tension ($[?] 600$ mN/m), and low toxicity while exhibiting a low viscosity of around 2.5 cP at room temperature.^[3,42] These properties and the ability to tune the physical properties, i.e., surface/interfacial tension, thermal conductivity, and rheological properties (viz., viscosity), as well as the ability to actuate and deform the liquid metals via ample methods, such as light, pH, chemical environment, and magnetic field, render them intriguing candidates for various applications, including high-precision manipulation, flexible electronics and soft robotics to drug delivery systems.^[2,49-52] For example, Xu et al.^[53] reported a kind of magnetic liquid droplet robot that can move due to a magnetic gradient field and this robot is able to perform cargo transfer and vessel cleaning. Sun et al.^[28] proposed a liquid metal-based robot that can jump in order to avoid obstacles, climb steep slopes, and rotate its body to the desired posture, and they anticipate application of this robot in targeted drug delivery. Liu et al.^[54] developed a magnetic liquid metal droplet, which can be stretched both horizontally and vertically, for electrode connections. Wang et al.^[55] proposed a ferrofluid comprising Ga and iron particles, and realized with it magnetic manipulation of non-magnetic objects via thermal switchable on-demand grasp and release enabled by the phase transition of the magnetic liquid metal composites. Although the deformability and mobility of the droplet-based robots have been advantageous for ample applications, it is still a challenge to fix complex droplet shapes against the intrinsic droplet shrinking towards a spherical and low interfacial energy state. Furthermore, most of the droplet-based robots offer only low electrical conductivity and the potential applications in transient electronics and circuit welding are rarely explored.

In this work, we designed and developed a liquid metal droplet-based soft robot with high electrical conductivity and excellent shape transformation ability based on magnetic actuation and infrared light triggered shape encoding (Figure 1a-1c). The soft robot comprises of liquid metal and carbonyl iron (iron pentacarbonyl) as magnetic particles. The thus obtained composite is used as a reconfigurable conductor in a circuit and serves as a switch, which can be controlled remotely. Under an external magnetic field, the soft robots, i.e., magnetic liquid metal composite, can perform multimodal movement, including reversible telescopic deformation, bending, and on-demand locomotion (Figure 1, Figure S1, Movie S1). In addition, the liquid metal droplet robots can also perform reversible coalescence and splitting by using specific magnetic fields. The telescopic and bending deformation of the liquid metal droplet robot can be exploited to realize selective interconnection and disconnection of electrodes in a complex circuit. Programmable shape encoding of the liquid metal robots and the phase transition of the robot between liquid and solid states can be utilized to fix a desired shape via cooling and localized infrared light irradiation. Furthermore, damaged circuits can be repaired by remote actuation, controllable coalescence, and on-demand circuit welding. In addition, the liquid metal can be fixed reversibly in a shape by cooling below the solidification temperature. Finally, the liquid metal composite utilized in this robot can be reclaimed and recycled. Therefore, this magnetic field responsive liquid metal-based soft robots are attractive devices as they expand the application scenarios of droplet-based soft robots toward on-demand circuit welding and transient and recyclable electronics.

2. Results and discussion

The magnetic liquid metal droplet was fabricated by simply mixing and grinding of carbonyl iron particles and Galinstan. Here, we use carbonyl iron particles instead of magnetite particles because they are easier to be wrapped and wetted by liquid metal (Figure S2). Figure 1d shows a photograph of a mortar filled with a mixture of carbonyl iron and particles Galinstan at a mass ratio of 2:8 after mixing. It should be noted that mixing of liquid metal with particles increases the viscosity and may alter the electrical conductivity of the resulting composite. The particle:liquid metal ratio was altered to elucidate the suitable amount of

added magnetic material. Figure 1e shows a series of liquid metal droplet robots with different particle and liquid metal mass ratios. At low mass ratios, i.e., 1:8 or 2:8, the composite behaves like a liquid and can be extruded from a syringe. However, at mass ratios greater than 2:8, the composite becomes more solid-like and can only be deformed plastically by exertion of an external force. These composites do not allow triggered break up and coalescence, as in this state, it is challenging to deform the plastic material. Moreover, particle aggregation results in loss of smoothness of the composite surface, which could adversely affect the locomotion of the composite. Furthermore, scanning electron microscopy (SEM) images show that the discontinuity of the composite increases with the proportion of particle in the liquid metal. At high carbonyl iron content, the magnetic particles show significant aggregation (Figure 1f-1j). The energy dispersive spectrometer (EDS) maps in Figure 1k and 1l show the distribution of the carbonyl iron powders and the liquid metal in the mixture. The EDS maps corroborate that at high particle content aggregation of particles is observed, as seen by several particle aggregates discernable in the EDS map, showing the location of Fe. Although a high amount of magnetic particles in the composite increases the force exerted on the composite by a magnetic field, the solid-like nature and increased roughness at mass ratios greater than 2:8 limit the applicability of the composite as shape morphing material. As a compromise between fluidity and sensitivity to an applied magnetic field, a mass ratio of 2:8 (carbonyl iron:Galinstan) was chosen to prepare the magnetic liquid composite.

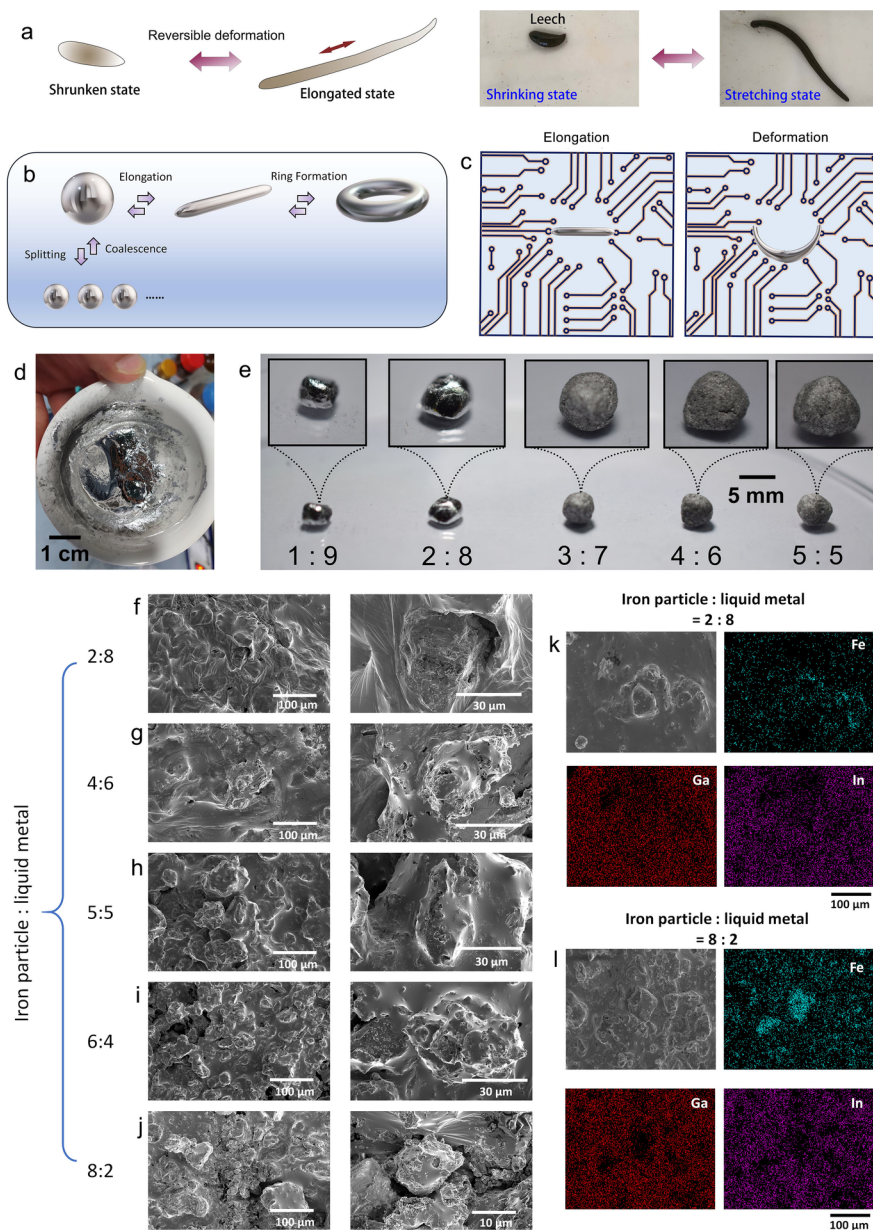


Figure 2: Figure 1. Leech-inspired liquid metal robots for reconfigurable circuit welding and transient electronics. (a) Schematic illustration and photographs showing the reversible shape transformation of a leech (Movie S1). (b) Schematic illustration showing the elongation, deformation, splitting, and coalescence of a liquid metal droplet robot. (c) Schematic illustration of an electronic circuit. In this circuit magnetic liquid metal is used as a reconfigurable conductor for the on-demand circuit welding. (d) Optical photograph a carbonyl iron:Galinstan composite (1:9 mass ratio) in a mortar after mixing. (e) Photographs of carbonyl iron:Galinstan composites at different mass ratios. In (d) and (e) the liquid metal was in contact with air. (f-j) SEM images showing the surface morphologies of the magnetic composites with different mass ratios. (k,l) EDS maps showing the uniformity of the distribution of carbonyl iron powder in the gallium indium tin alloy matrix at low (k) and high (l) mass ratios.

The liquid metal-based soft robotic platform consists of the abovementioned liquid and magnetic composite

and an external magnetic field setup (a permanent magnet but an electromagnetic can in principle also be used). Initially, a bar magnet was used to characterize shape transformation of the composite and exerted field strength to the composite. The bar magnet was positioned below an acrylic sheet. The liquid metal composite was placed on the acrylic sheet surrounded by water, in order to mitigate adhesion of the oxide layer of the liquid metal. The resistance to adhesion can be ascribed to a slip layer between acrylic sheet and the liquid metal-based robot (oxide skin).^[56] A scheme of the experimental setup can be viewed in Figure 2a. The simulation result in Figure 2b describes the magnetic field distribution around the bar magnet. More specifically, the magnetic field distribution of the planes at certain distances along the vertical axis are shown in Figure 2c. The strong magnetic field strength along the bar magnet is the driving force for the elongation of the liquid metal droplet robots. For example, with a bar magnet, gradually increasing the field strength H and the vertical gradient dH/dz acting on the droplet (by decreasing the gap between the magnet and the liquid metal droplet) leads to variation of the length of the composite robot, as shown in Figure 2d. In contrast, by using a circular permanent magnet, the composite forms a semi-circular conductor. Importantly, the elongation of the composite can be modulated by the distance between the LM composite and the bar magnet. At long distance between the composite and the bar magnet, the liquid metal exhibits a spherical shape (due to interfacial tension) and the marginal pulling force of the magnetic field exerted on the magnetic particles in the composite (first image in Figure 2d). Upon decreasing the distance, the pulling force (field strength of the bar magnet, as shown in Figure 2e) gets greater and deformation of the droplet toward a liquid metal line can be observed. This deformation gets more pronounced the higher the field strength gets. Interestingly, the shape transformation can be reversed by slowly removing the bar magnet (Figure 2d). The observed stretching and curl up of the composite resemble the shape change of a leech. In Figure 2f, the length of the composite is plotted versus the magnetic field strength. Initially, the LM composite is shaped ovaloid with a length of around 6.8 mm and a height of 1.6 mm. Upon application of the magnetic field, the composite elongates to around 22-23 mm at 100 - 160 mT, which is ascribed to the pulling force of the bar magnet's magnetic field. Upon converging of the bar magnet and the composite, the field strength rises to 200 mT and the length increases further to 25 mm. Thus, a 3.5-fold increase in length can be achieved by this means.

Importantly, this approach is not limited to shape transformation into elongated structures, but can also be used to generate bend structures, as shown in the scheme in Figure 2h. To generate a circular composite conductor pattern on a surface, a circular magnet can be used. The circular magnet generates a magnetic field with a strong field strength above its circular shape and forms a weak magnetic field at the circular center, resulting in bending of the liquid metal droplet robots (Figure 2h and i). Upon rotating the circular magnet along the vertical axis of its diameter, a circular conductive trace is generated on the acrylic substrate, as shown in Figure 2j. This shape morphing is interesting as we show later that the shape transformation is reversible. Generally, the extend of shape transformation achievable by this means is greater for a bigger composite droplet, and droplets with a volume of 50 μL or above work well.

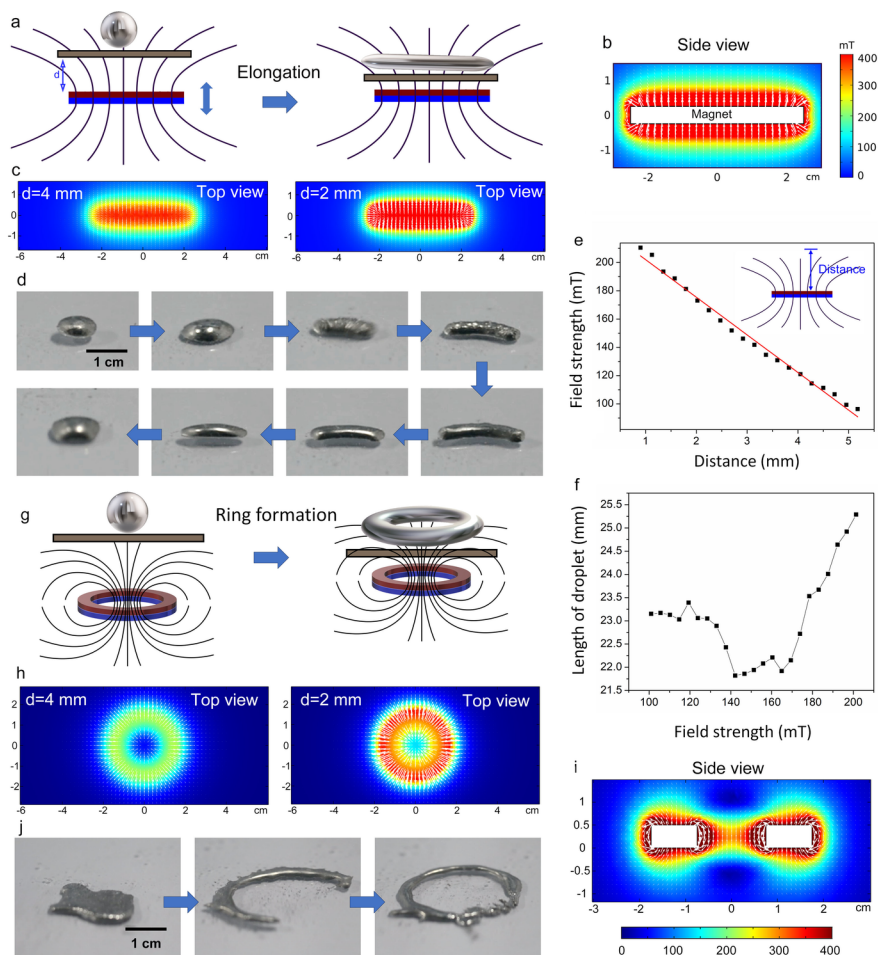


Figure 3: Figure 2. Controlled deformation of the liquid metal droplets. (a) Schematic illustration of the magnetic field-controlled elongation of the liquid metal droplet robot in water on an acrylic substrate. (b) Simulation result showing the magnetic field distribution of a bar magnet with the size of $5 \times 1 \times 0.5 \text{ cm}^3$ (Side view). (c) Simulation result showing the magnetic field distribution of a bar magnet ($5 \times 1 \times 0.5 \text{ cm}^3$) at the distance of 4 mm and the distance of 2 mm (Top view). (d) Magnetic field-induced reversible elongation and deformation of a liquid metal soft robot upon manipulation of the magnetic field by the distance of a bar magnet. (e) Dependence of the magnetic field strength on the distance between the bar magnet and the sample. (f) Dependence of the length of a composite droplet on the magnetic field strength. The initial length and height were 6.8 mm and 1.6 mm, respectively. (g) Schematic illustration of the generation of a circular conductor via converging of a circular and permanent magnet to an LM composite on acrylic substrate, followed by rotating the magnet. (h) Simulation result showing the magnetic field distribution of a circular magnet (outer diameter is 3.5 cm, inner diameter is 1.5 cm, height is 0.5 cm) at the distance of 4 mm and the distance of 2 mm (Top view). (i) Simulation result showing the magnetic field distribution of a circular magnet (side view). (j) Optical photographs of the shape transformation of a composite puddle into a semi-circle and a circle, as shown schematically in (g).

Not limited to shape transformation, the liquid metal can also be reversibly split up into several smaller liquid metal droplets by magnetic field actuation. This is achieved by a setup similar to the one shown in Figure 2g and S3. However, the circular magnet is not rotated along the vertical axis of the diameter of the ring magnet, but along the horizontal axis. Upon such a rotation and control of the distance between the

composite and the magnet, the droplet robot gradually deforms (elongates) and finally splits into composite droplets, as shown schematically in Figure 3a. The simulation result in Figure 3b gives the variation of the magnetic field distribution before and after rotation. Splitting of a bigger droplet into 2, 3, and 8 droplets is shown in Figure 3c, 3d, and 3e, respectively (Movie S2). During the splitting process, one can observe the morphology change of the droplet surface because of the formed particle chains inside the droplet. The particle chains are generated by the dipole attractive forces under the magnetic field (as shown in Figure S4). (1) When the diameter of the liquid metal droplet is substantially larger than the characteristic size of the particle chains, the morphology of the liquid metal droplets before and after splitting will be consistent without obvious change. (2) When the diameter of liquid metal droplet is comparable with or even smaller than the characteristic size of the particle chains, the morphology of the liquid metal droplets will be affected by the incorporated particle chains. The splitting of the liquid metal droplet is due to a combination of high magnetic field strength and high vertical magnetic field gradient, which cannot be achieved with uniform magnetic fields. To trigger splitting of the liquid metal droplet (gravitational force of the droplet here is negligible compared with the magnetic force), the droplet diameter (D) should be larger than the critical wavelength of the Rosensweig pattern (λ_C , Figure S5).^[38,57]

$$D > \lambda_C \approx 2\pi \sqrt{\frac{\sigma}{\frac{d}{dz}(\mu_0 H M)}}$$

where σ is the surface tension of the liquid, μ_0 is the permeability of vacuum, and M is the magnetization. In our experiment, larger liquid metal droplets are much more susceptible to splitting. The droplet size of the split droplets appears to be comparable. Furthermore, the split droplets can be split again to obtain more magnetically moveable composite droplets. Thus, on demand breakup and disassembly of a robot into many smaller robots is achieved, which renders this approach useful to perform highly complex and sophisticated tasks.

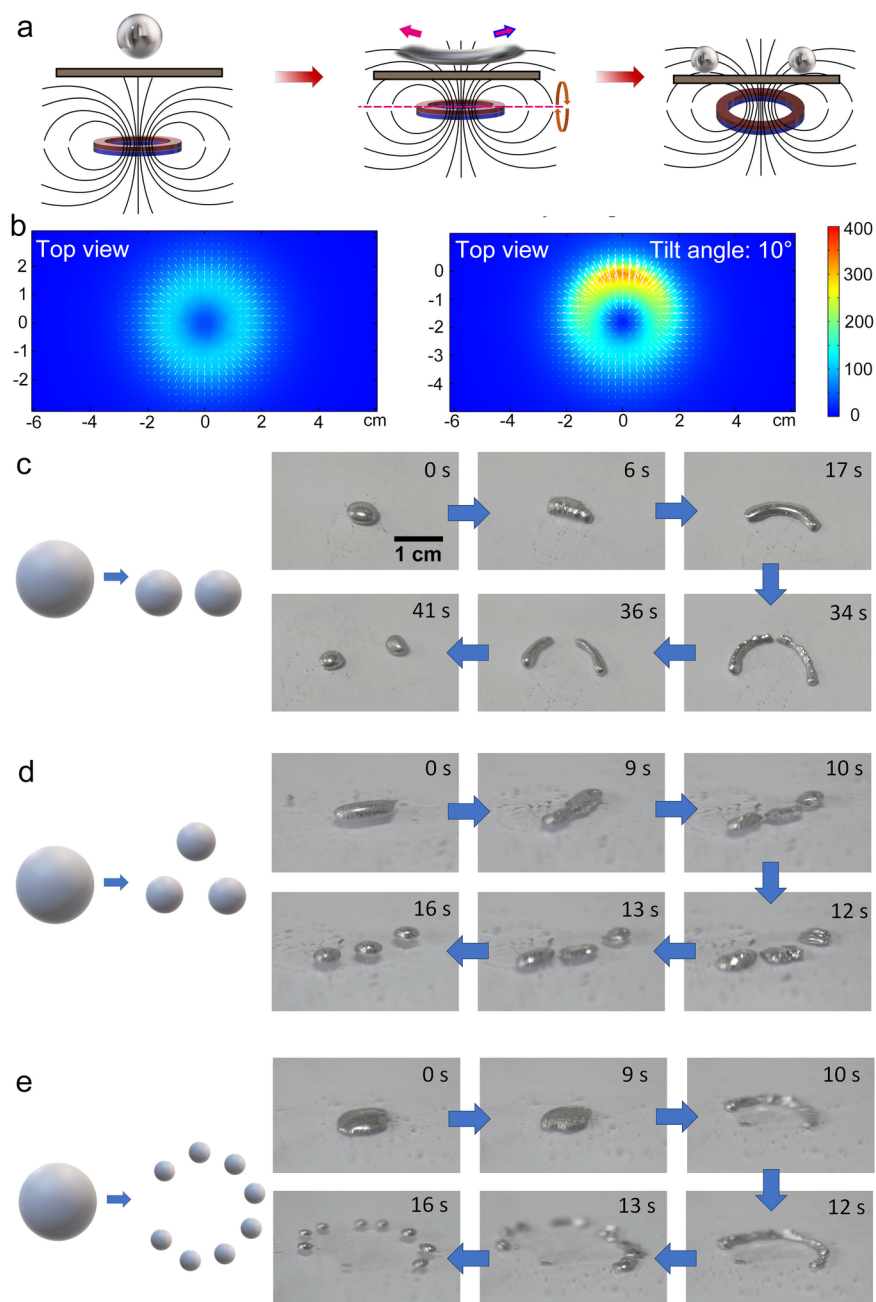


Figure 3. On-demand splitting of the LM composite robots. (a) Schematic illustration of the on-demand splitting of the LM composite robots by the use of a circular magnet. (b) Simulation result showing the magnetic field distribution of a circular magnet (outer diameter is 3.5 cm, inner diameter is 1.5 cm, height is 0.5 cm) before and after rotation (Top view). (c-e) Photographs of the splitting process of the liquid metal soft robot into separate sub-droplets on an acrylic sheet filled with alkaline water: (c) two sub-droplets, (d) three sub-droplets, and (e) eight sub-droplets.

Importantly, the on-demand splitting of the LM composite robots is reversible. To trigger the coalescence process of liquid metal droplets, the system should overcome the energy barrier between two liquid metal

droplets that are generated by the surface oxide layer. The oxide layer is in our case removed by the alkaline medium. Afterwards, the coalescence process is a spontaneous process because the liquid metal droplets tend to shrink into spherical shape so as to minimize the surface energy. Upon moving two or more droplets together they merge (coalesce), which is fueled by the high interfacial tension of the liquid metal (and liquid metal oxide), as shown schematically in Figure 4a. Here, the droplets are steered and actuated by a bar magnet located below the acrylic sheet. Upon converging of the two droplets in Figure 4a, the LM-based robots quickly coalesce and the coalescence process is completed in less than 1 second. Moreover, the coalescence of several droplets (see Figure 4b, Movie S3), an array of droplets (see Figure 4c), and a pattern (see Figure 4d) can be done swiftly due to the good precision of the magnetic actuation and the quick coalescence kinetics. This process can be leveraged to remove and recycle the liquid metal-based robots to a high degree.

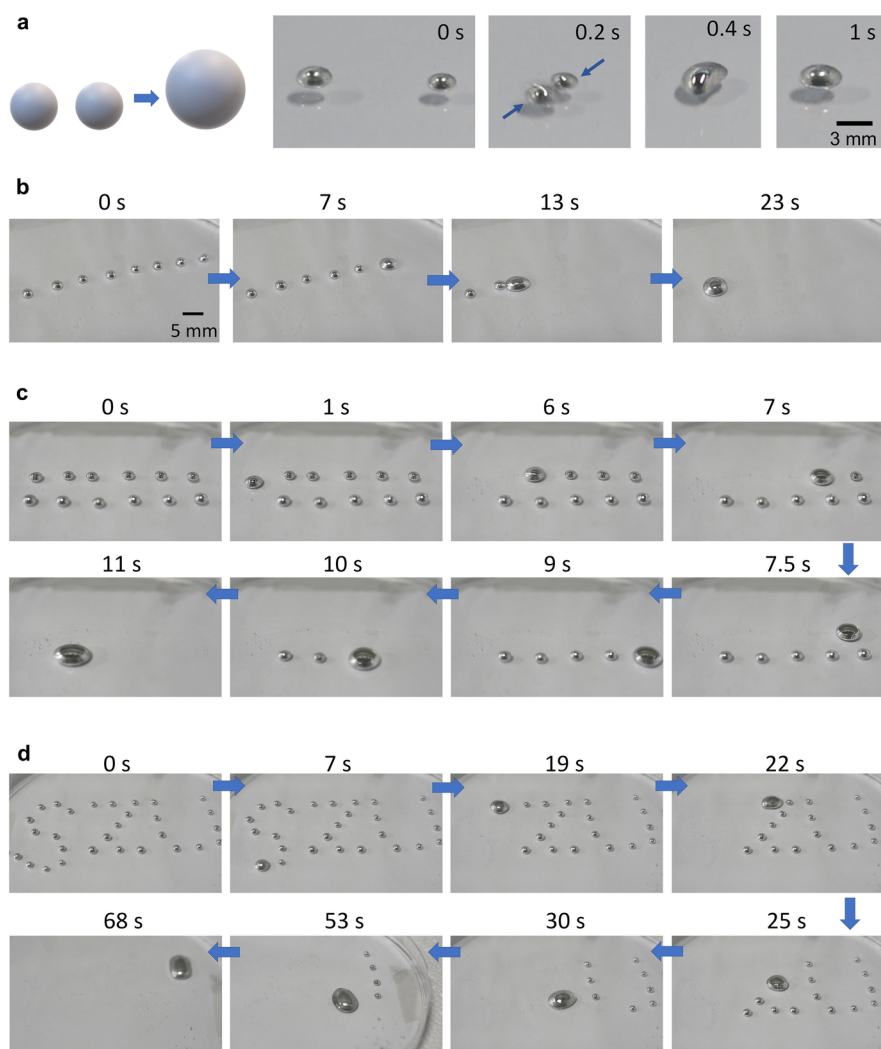


Figure 5: Figure 4. Coalescence of liquid metal-based soft robots. (a) Scheme and photographs of merging droplet robots. (b) Coalescence of liquid metal droplets in a line pattern. (c) Coalescence of liquid metal droplets in a rectangular array pattern. (d) Merging of liquid metal droplets, which are arranged to signify the letters S, Z, and U. The surrounding medium is in these experiments alkaline water.

The control of the droplet shape is not limited to elongation, bending, and on-demand droplet splitting and merging. Patterns can even be achieved on a surface without a necessitating a water layer by first elongating a droplet with a centimeter-sized bar magnet on a superhydrophobic and liquid metal phobic (lyophobic) surface (SEM images of the surface morphology is given in Figure S6), followed by magnetically steering of one end of the elongated liquid metal-based robot with the tip of the bar magnet, as schematically shown in Figure 5a. In general, the oxide skin of gallium-based liquid metal is considered to be sticky and actuation on dry medium is therefore difficult. Adhesion of liquid metal in such an instance can be avoided by decorating the liquid metal with nano-/microparticles. Yet, this would not be conducive in this experiment, as the deformation would generate new surfaces, which would be exposed and could adhere to the surface. The role of the liquid metal phobic surface is to reduce friction and adhesion of the surface towards the soft robots by reduced contact area (viz., by roughness) in combination with the solid-like behavior of the oxide skin.^[58,59] Due to the oxide layer on the robot surface, which exhibits a yield stress, the droplet maintains the shape after the bar magnet is removed. Figure 5b signifies that the liquid metal-based robots can be steered. For example, it is feasible to draw Arabic numbers 1 to 10, and thus, this method offers a general way to deform the liquid metal droplet into complex shapes in a reconfigurable and reversible fashion, which can be leveraged for dynamically reconfigurable and recyclable switches in complex circuits and electronics. Moreover, the phase transition temperature of the liquid metal can be exploited to fix a desired shape after the programmable shape encoding.

Finally, the phase transition temperature of the liquid metal (Gallium) can be exploited to fix a desired shape or interconnection. For example, a connection can be established at room temperature, followed by freezing the liquid metal in place (which results in a highly increase modulus (solid state)). Once reconfiguration gets necessary, the robot can be melted, yielding the soft and reconfigurable state again (Figure 5d, Movie S4). To change the melting and solidification temperature, Ga can be alloyed with In and Sn to reduce the melting temperature or Cu to increase the melting temperature.^[60]

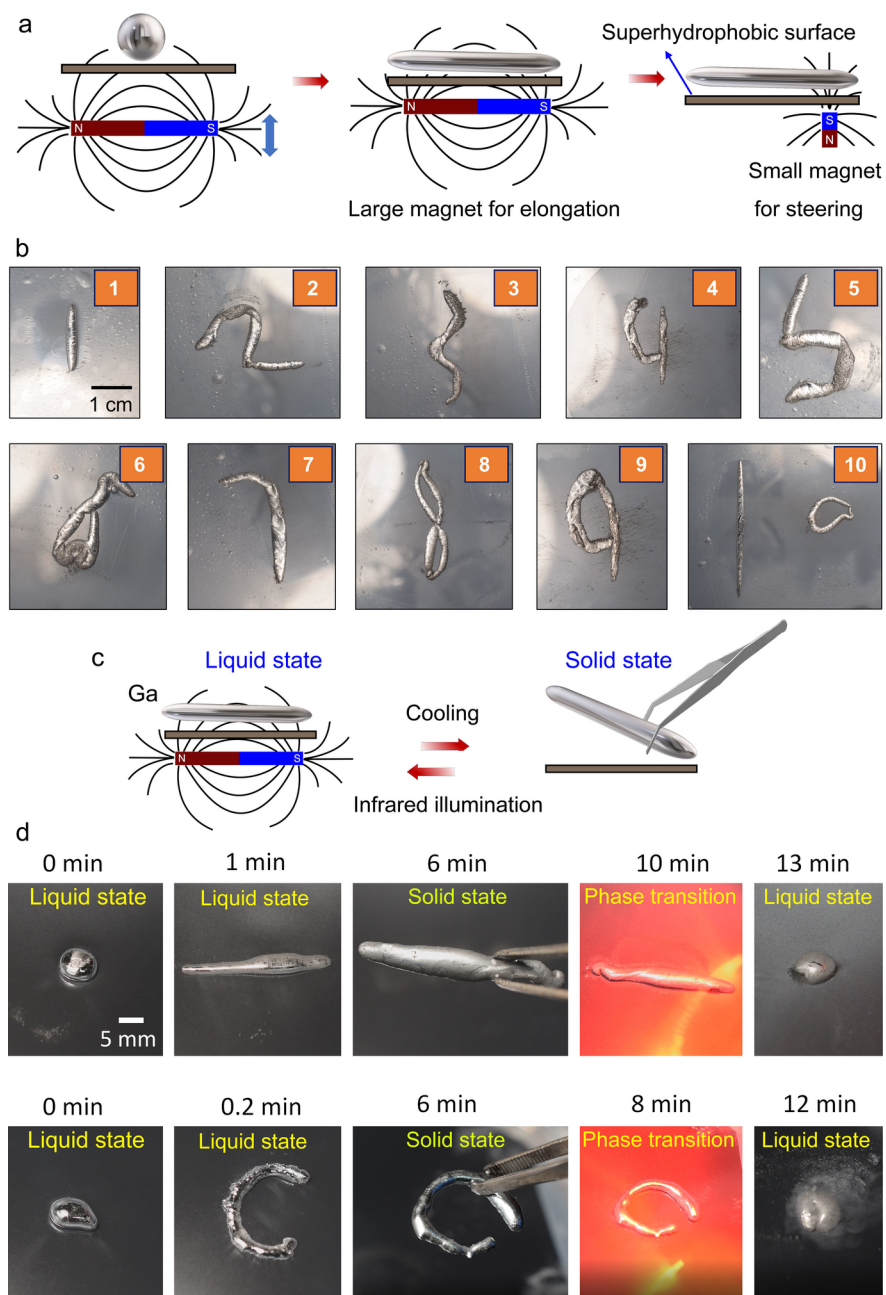


Figure 5. Reversible phase transition of the liquid metal droplet robot between liquid state and solid state. (a) Schematic showing the magnetic field-controlled deformation of the liquid metal-based droplet robot in order to achieve different patterns. The robot is surrounded by air and located on a hydrophobic (spray coated) petri dish. (b) Photographs of the magnetic field-controlled deformation of the liquid metal droplet robot into the numbers 1 to 10. The experiment is performed on a liquid metal lyophobic surface. (c) Schematic showing the reversible phase transition of the liquid metal (Gallium) droplet robot between liquid state and solid state. (d) Photographs of the reversible phase transition of the liquid metal droplet robot between liquid state and solid state with different patterns generated by magnetic field on a silicon surface (SEM images of the surface morphology of the silicon surface is given in Figure S7, Movie S4).

The good deformability and electrical conductivity of the liquid metal-based soft robot enable its application as a miniature electronic switch, which can be remotely controlled. A circuit comprising 3 LED arrays that depict the letters “S”, “Z”, and “U” and copper foil as interconnects in a water bath (with 1 wt% Tween 80). Each of the LED arrays has its own open circuit, as depicted in Figure 6a (Movie S5). The copper electrodes in the water bath do not touch each other, resulting in an open circuit. Here, the liquid metal-based soft robot is employed as a controllable switch; the deformation and shape morphing are controlled by a magnet. Initially, all circuits were open and the LED arrays remained dark. After placing a liquid metal-based soft robot in the middle of the electrodes and actuating it by a bar magnet, one of the three open circuits (the one connected to the “S” LED array) was closed, resulting in the light-up of the “S” LED array, as shown in Figure 6b. Similarly, other LED arrays can be selectively switched on and off again. Furthermore, one single soft robot could be deformed circular, as described 3e and f, in order to close all three circuits, resulting in light up of all three LED arrays, which spell together the acronym SZU (see Figure 6c). Importantly, the on-demand deformation of the liquid metal-based soft robot is reversible and other interconnection patterns can quickly be achieved. Furthermore, the soft robot can be retrieved after usage and reused for other applications. These results demonstrate the capability of the liquid metal-based soft robots and their potential in applications like dynamic and recyclable switches for complex circuits. Compared with a traditional miniature electronic switch, which may require a complex switch design or multiple switches to control the complicated circuit, the liquid metal droplet robots enable simple remote control of complex circuits in a reconfigurable manner, which effectively simplifies the circuit layout.

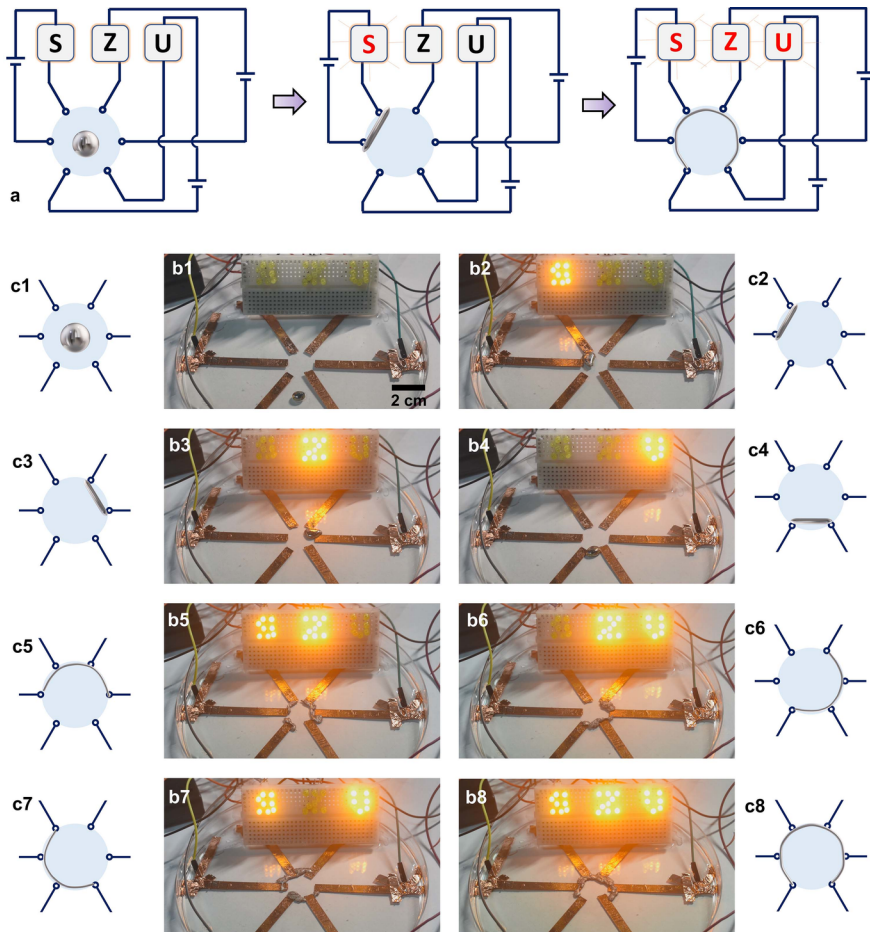


Figure 7: **Figure 6. Reconfigurable circuit welding and transient electronics.** (a) Schematic showing the circuit connected to the LEDs spelling ‘SZU’. The liquid metal robot serves as a reconfigurable interconnector. The experiment is done in a petri dish filled with a thin layer of water (Movie S5). (b1-b8) Optical images of the actual circuit. The light is turned on or off by the droplet in the center of the control platform. (c1-c8) Schematic diagrams of the circuit corresponding to the photographs in (b1-b8).

Liquid metal-based soft materials (hydrogels and elastomers) are capable of self-healing and restoring electrical functionality by magnetic field or even spontaneously, exhibiting uncompromising resilience to mechanical damage.^[61-63] Here, Liquid metal soft robots can also be used to repair damaged microcircuits that occur at an unreachable space in a non-invasive manner. A maze was used to simulate an unreachable area, and multiple liquid metal-based soft robots are actuated towards the damaged section of the circuit. After reaching the damaged section of the circuit, the soft robots were fused and deformed by actuation with a bar magnet. Finally, the damaged section was successfully repaired (~6 min). A schematic illustration of such a process is shown in Figure S8. In Figure S8, the optical photographs of the movement (through the maze) and repairing process are shown, signifying the high control and potential of such soft robots. For instance, the soft robots can solve the maze and circumvent obstacles with ease without necessitating the use of an electric field and conductive electrolyte (compare with ^[64]).

Due to the fluidity of the liquid metal matrix, the liquid metal soft robot has a high degree of freedom of shape changeability, which endows it with the ability to adapt to the working environment, i.e., confined space. In channels with different widths, the liquid metal soft robot can adaptively change its shape and

move in an optimized low-resistance mode. The self-adaptability of the shape enables the liquid metal soft robot to maintain good mobility in various environments.

3. Conclusion

A magnetic field-actuated liquid metal-based droplet robot was designed and developed that can be applied for reconfigurable and transient electronics, i.e., as a remote-controlled circuit switch. These robots comprise of the liquid metal and the magnetic particle iron pentacarbonyl. Upon exertion of an external magnetic field (by a permanent magnet), the magnetic liquid metal-based soft robot can undergo reversible elongation, bending, and on-demand locomotion. Programmable shape encoding of the liquid metal robots and the phase transition of the robot between liquid and solid states can be utilized to fix a desired shape via ice cooling and infrared light irradiation. Furthermore, on-demand merging and splitting up of the soft robots can be achieved by controlling the direction and shape of the electric field. The on-demand elongation and bending of the soft robots was used in a dynamic and recyclable switch in a complex circuit. Compared with traditional miniature electronic switches, the liquid metal droplet robot enables simple and remote control of the complex circuits in a reconfigurable manner, which effectively simplifies the circuit layout. In addition, the liquid metal soft robot can be removed and recycled by removing the robot with the help of the magnetic field. In this case, the open circuit is regained together with the reusable soft robot. Besides, multiple liquid metal droplet robots can repair damaged sections of microcircuits by remote actuation, controllable coalescence, and on-demand circuit welding. The technology provides a new application scenario of droplet-based soft robots for on-demand circuit welding and transient recyclable electronics.

4. Materials and Methods

Materials

Gallium-indium-tin (Galinstan, Ga 68.5 wt%, In 21.5 wt%, Sn 10 wt%, density: 6.44 kg/L) alloy and Gallium were purchased from Wochang (P. R. China). Carbonyl iron (iron pentacarbonyl, size $\sim 2 \mu\text{m}$) powder was purchased from BASF. Tween 80 was purchased from Aladdin. As water source deionized water (DI water) was used. The experimental materials were used as received without any further purification and treatment.

Preparation of the magnetic liquid metal composite

Certain masses of carbonyl iron powder and Galinstan/Gallium were balanced according to the mass ratio in the experiment (typically 2:8; particle:liquid metal). The two materials were mixed by grinding with a mortar and pestle. Afterwards, slow (60~90 rpm) mechanical stirring was employed for 20 min to homogenize the mixture.

Preparation of the liquid metal droplet robot:

To prepared millimeter-scale droplets, a certain amount of magnetic liquid metal is slowly extruded in a tank pre-filled with water/surfactant (tween 80, $\sim 1\%$ in weight) solution. For microscale droplets, the liquid metal is extruded rapidly on a water bath.

Magnetic control platform:

The magnetic field setup consists of a strong permanent magnet (bar magnet or circular magnet), which is located under the mobile platform and moves by manual control in the x-y and z plane. Based on the orientation and strength of the magnetic field, the liquid metal soft robot is controlled. To control the strength of the magnetic field (magnet) exerted toward the execution unit (liquid metal soft robot) the relative distance (d) between the magnet and the liquid metal soft robot is important and needs to be adjusted.

Based on the difference of the initial d value, the control method can be divided into two types:

1. Precision operation. The initial value of d is small ($d < 2 \text{ mm}$). Upon exertion of a strong magnetic field, the liquid metal soft robot establishes a stable connection with the magnet. Within a certain speed range,

the liquid metal soft robot moves or deforms with the movement of the magnet. This kind of control method is suitable for precision operation, elongation, and bending of the droplet robot.

2. Quick movement. The initial value of d is large ($d > 50$ mm). The distance d is gradually reduced, and the ability to control the droplet is increased. When d decreases below the threshold distance, the liquid metal soft robot moves toward the magnet rapidly until the liquid metal soft robot is closely connected with the magnet through magnetic force and enters the precision operation mode. This control method is suitable for the rapid movement of liquid metal soft robots.

Characterization

Scanning electron microscopy (SEM) images and the EDS mappings were obtained from the APREO S (Thermo Scientific).

Acknowledgment

This work was supported by the National Natural Science Foundation of China (22102104, 21922303), Natural Science Foundation of Shenzhen University with grant No. 000002110712, Natural Science Foundation of Shenzhen Science and Technology Commission with grant No. RCBS20200714114920190, Guangdong Basic and Applied Basic Research Foundation (2020B1515020045 and 2021A1515010672), and Shenzhen Municipality Science and Technology Planning Project (SGLH20180622151607182, KQJSCX20170727100240033).

Declaration of Competing Interest

The authors declare that they have no known competing financial interests.

References

- [1] C. Kaspar, B. J. Ravoo, W. G. van der Wiel, S. V. Wegner and W. H. P. Pernice, The rise of intelligent matter. *Nature*, vol. 594, pp. 345-355, 2021.
- [2] M. Medina-Sánchez, V. Magdanz, M. Guix, V. M. Fomin and O. G. Schmidt, Swimming microrobots: Soft, reconfigurable, and smart. *Adv. Funct. Mater.*, vol. 28, article 1707228, 2018.
- [3] B. Wang, K. F. Chan, K. Yuan, Q. Wang, X. Xia, L. Yang, H. Ko, Y. Wang, J. J. Y. Sung, P. W. Y. Chiu and L. Zhang, Endoscopy-assisted magnetic navigation of biohybrid soft microrobots with rapid endoluminal delivery and imaging. *Sci. Robot.*, vol. 6, article eabd2813, 2021.
- [4] Y. Yan, Z. Hu, Z. Yang, W. Yuan, C. Song, J. Pan and Y. Shen, Soft magnetic skin for super-resolution tactile sensing with force self-decoupling. *Sci. Robot.*, vol. 6, article eabc8801, 2021.
- [5] X. Yang, W. Shang, H. Lu, Y. Liu, L. Yang, R. Tan, X. Wu and Y. Shen, An agglutinate magnetic spray transforms inanimate objects into millirobots for biomedical applications. *Sci. Robot.*, vol. 5, article eabc8191, 2020.
- [6] X. Hu, I. C. Yasa, Z. Ren, S. R. Goudy, H. Ceylan, W. Hu and M. Sitti, Magnetic soft micromachines made of linked microactuator networks. *Sci. Adv.*, vol. 7, article eabe8436, 2021.
- [7] M. Sitti, H. Ceylan, W. Hu, J. Giltinan, M. Turan, S. Yim and E. Diller, Biomedical Applications of Untethered Mobile Milli/Microrobots. *Pro. IEEE*, vol. 103, pp. 205-224, 2015.
- [8] B. Shih, D. Shah, J. Li, T. G. Thuruthel, Y.-L. Park, F. Iida, Z. Bao, R. Kramer-Bottiglio, M. T. Tolley, Electronic skins and machine learning for intelligent soft robots. *Sci. Robot.*, vol. 5, article aaz9239, 2020.
- [9] F. Ji, B. Wang and L. Zhang, Light-Triggered Catalytic Performance Enhancement Using Magnetic Nanomotor Ensembles. *Research*, vol. 2020, article 6380794, 2020.
- [10] Q. Wang, K. Chan, K. Schweizer, X. Du, D. Jin, S. C. H. Yu, B. J. Nelson and L. Zhang, Ultrasound Doppler-guided real-time navigation of a magnetic microswarm for active endovascular delivery. *Sci. Adv.*, vol. 7, article eabe5914, 2021.

- [11] J. F. Boudet, J. Lintuvuori, C. Lacouture, T. Barois, A. Deblais, K. Xie, S. Cassagnere, B. Tregon, D. B. Brückner, J. C. Baret and H. Kellay, From collections of independent, mindless robots to flexible, mobile, and directional superstructures. *Sci. Robot.*, vol. 6, article eabd0272, 2021.
- [12] C. Xu, Z. Yang, G. Z. Lum, Small-Scale Magnetic Actuators with Optimal Six Degrees-of-Freedom. *Adv. Mater.*, vol. 33, article 2100170, 2021.
- [13] D. Rus and M. T. Tolley, Design, fabrication and control of soft robots. *Nature*, vol. 521, pp. 461-475, 2015.
- [14] A. M. Petersen, W. Chin, K. L. Feilich, G. Jung, J. L. Quist, J. Wang and D. J. Ellerby, Leeches run cold, then hot. *Biol. Lett.*, vol. 7, pp. 941-943, 2011.
- [15] L. Zheng, S. Handschuh-Wang, Z. Ye and B. Wang, Liquid metal droplets enabled soft robots. *Appl. Mater. Today*, vol. 27, article 101423, 2022.
- [16] S. M. Mirvakili, D. Sim, I. W. Hunter and R. Langer, Actuation of untethered pneumatic artificial muscles and soft robots using magnetically induced liquid-to-gas phase transitions. *Sci. Robot.*, vol. 5, article eaaz4239, 2020.
- [17] H. Wang, Y. Yao, X. Wang, L. Sheng, X. Yang, Y. Cui, P. Zhang, W. Rao, R. Guo, S. Liang, W. Wu, J. Liu and Z. He, Large-Magnitude Transformable Liquid-Metal Composites. *ACS Omega*, vol. 4, pp. 2311–2319, 2019.
- [18] B. Wang, K. Kostarelos, B. J. Nelson and L. Zhang, Trends in Micro-/Nanorobotics: Materials Development, Actuation, Localization, and System Integration for Biomedical Applications. *Adv. Mater.*, vol. 33, article 2002047, 2021.
- [19] L. Zhu, B. Wang, S. Handschuh-Wang and X. Zhou, Liquid Metal–Based Soft Microfluidics. *Small*, vol. 16, article 1903841, 2019.
- [20] A. Li, H. Li, Z. Li, Z. Zhao, K. Li, M. Li and Y. Song, Programmable droplet manipulation by a magnetic-actuated robot. *Sci. Adv.*, vol. 6, article eaay5808, 2020. [21] Y. Si, J. Hu and Z. Dong, Bioinspired magnetically driven liquid manipulation as microrobot. *Cell Rep. Phys. Sci.*, vol. 2, article 100439, 2021.
- [22] B. Wang, K. F. Chan, F. Ji, Q. Wang, P. W. Y. Chiu, Z. Guo and L. Zhang, On-Demand Coalescence and Splitting of Liquid Marbles and Their Bioapplications. *Adv. Sci.*, vol. 6, article 1802033, 2019.
- [23] D. Sun, D. Zhou, Y. Gao, H. Yue, W. Wang, X. Ma and L. Li, Phototaxis Motion Behavior of a Self-propelled Submarine-like Water Droplet Robot in Oil Solvent. *ChemNanoMat*, vol. 6, pp. 1611-1616, 2020.
- [24] X. Fan, X. Dong, A. C. Karacakol, H. Xie and M. Sitti, Reconfigurable multifunctional ferrofluid droplet robots. *Proc. Natl. Acad. Sci. U. S. A.*, vol. 117, pp. 27916-27926, 2020.
- [25] D. Chen, Z. Yang, Y. Ji, Y. Dai, L. Feng and F. Arai, Deformable ferrofluid-based millirobot with high motion accuracy and high output force. *Appl. Phys. Lett.*, vol. 118, article 134101, 2021.
- [26] Q. Wang, L. Yang, B. Wang, E. Yu, J. Yu and L. Zhang, Collective Behavior of Reconfigurable Magnetic Droplets via Dynamic Self-Assembly. *ACS Appl. Mater. Interfaces*, vol. 11, pp. 1630-1637, 2019.
- [27] J. Zhang, Y. Yao, L. Sheng and J. Liu, Self-Fueled Biomimetic Liquid Metal Mollusk. *Adv. Mater.*, vol. 27, pp. 2648-2655, 2015.
- [28] F. Li, J. Shu, L. Zhang, N. Yang, J. Xie, X. Li, L. Cheng, S. Kuang, S. Tang, S. Zhang, W. Li, L. Sun and D. Sun, Liquid metal droplet robot. *Appl. Mater. Today*, vol. 19, article 100597, 2020.
- [29] Y. Wang, W. Duan, C. Zhou, Q. Liu, J. Gu, H. Ye, M. Li, W. Wang and X. Ma, Phoretic Liquid Metal Micro/Nano-Motors as Intelligent Filler for Targeted Micro-Welding. *Adv. Mater.*, vol. 31, article 1905067, 2019.

- [30] J. Wu, S. Tang, T. Fang, W. Li, X. Li and S. Zhang, A Wheeled Robot Driven by a Liquid-Metal Droplet. *Adv. Mater.*, vol. 30, article 1805039, 2018.
- [31] E. Wang, J. Shu, H. Jin, Z. Tao, J. Xie, S. Tang, X. Li, W. Li, M. Dickey and S. Zhang, Liquid metal motor. *iScience*, vol. 24, article 101911, 2021.
- [32] D. Wang, C. Gao, W. Wang, M. Sun, B. Guo, H. Xie and Q. He, Shape-Transformable, Fusible Rodlike Swimming Liquid Metal Nanomachine. *ACS Nano*, vol. 12, pp. 10212, 2018.
- [33] Z. Li, H. Zhang, D. Wang, C. Gao, M. Sun, Z. Wu and Q. He. Reconfigurable Assembly of Active Liquid Metal Colloidal Cluster. *Angew. Chem. Int. Ed.*, vol. 59, pp. 19884-19888, 2020.
- [34] Z. Li, H. Zhang, Z. Wu and Q. He, Acoustically-Propelled Rodlike Liquid Metal Colloidal Motors. *ChemNanoMat*, vol. 7, pp. 1-6, 2021.
- [35] X. Li, S. Li, Y. Lu, M. Liu, F. Li, H. Yang, S. Tang, S. Zhang, W. Li and L. Sun, Programmable Digital Liquid Metal Droplets in Reconfigurable Magnetic Fields. *ACS Appl. Mater. Interfaces*, vol. 12, pp. 37670–37679, 2020.
- [36] Z. Lin, C. Gao, D. Wang and Q. He, Bubble-Propelled Janus Gallium/Zinc Micromotors for the Active Treatment of Bacterial Infections. *Angew. Chem. Int. Ed.*, vol. 60, pp. 8750-8754, 2021.
- [37] S. Y. Tang, K. Khoshmanesh, V. Sivan, P. Petersen, A. P. O'Mullane, D. Abbott, A. Mitchell and K. Kalantar-zadeh, Liquid metal enabled pump. *Proc. Natl. Acad. Sci. U. S. A.*, vol. 111, pp. 3304-3309, 2014.
- [38] J. V. Timonen, M. Latikka, L. Leibler, R. H. Ras and O. Ikkala, Switchable static and dynamic self-assembly of magnetic droplets on superhydrophobic surfaces. *Science*, vol. 341, pp. 253–257, 2013.
- [39] X. Liu, N. Kent, A. Ceballos, R. Streubel, Y. Jiang, Y. Chai, P. Y. Kim, J. Forth, F. Hellman, S. Shi, D. Wang, B. A. Helms, P. D. Ashby, P. Fischer and T. P. Russell, Reconfigurable ferromagnetic liquid droplets. *Science*, vol. 365, pp. 264–267, 2019.
- [40] A. M. Mullis, K. I. Dragnevski and R. F. Cochrane, The solidification of undercooled melts via twinned dendritic growth. *Mater. Sci. Eng. A*, vol. 375–377, pp. 547-551, 2004.
- [41] S. Handschuh-Wang, L. Zhu, T. Gan, T. Wang, B. Wang and X. Zhou, Interfacing of surfaces with gallium-based liquid metals – approaches for mitigation and augmentation of liquid metal adhesion on surfaces. *Appl. Mater. Today*, vol. 21, article 100868, 2020.
- [42] M. D. Dickey, Stretchable and Soft Electronics using Liquid Metals. *Adv. Mater.*, vol. 29, article 1606425, 2017.
- [43] K. Kim, Y.-G. Park, B. G. Hyun, M. Choi and J.-U. Park, Recent Advances in Transparent Electronics with Stretchable Forms. *Adv. Mater.*, vol. 31, article 1804690, 2019.
- [44] T. Daeneke, K. Khoshmanesh, N. Mahmood, I. A. de Castro, D. Esrafilzadeh, S. J. Barrow, M. D. Dickey and K. Kalantar-zadeh, Liquid metals: fundamentals and applications in chemistry. *Chem. Soc. Rev.*, vol. 47, pp. 4073-4111, 2018.
- [45] K. Khoshmanesh, S.-Y. Tang, J. Y. Zhu, S. Schaefer, A. Mitchell, K. Kalantar-Zadeh and M. D. Dickey, Liquid metal enabled microfluidics. *Lab Chip*, vol. 17, pp. 974-993, 2017.
- [46] S. Handschuh-Wang, T. Gan, T. Wang, F. Stadler and X. Zhou, Surface Tension of the Oxide Skin of Gallium-Based Liquid Metals. *Langmuir*, vol. 37, pp. 9017-9025, 2021.
- [47] G. Wilde, J. L. Sebright and J. H. Perepezko, Bulk liquid undercooling and nucleation in gold. *Acta Mater.*, vol. 54, pp. 4759-4769, 2006.
- [48] M. D. Dickey, R. C. Chiechi, R. J. Larsen, E. A. Weiss, D. A. Weitz and G. M. Whitesides, Eutectic Gallium-Indium (EGaIn): A Liquid Metal Alloy for the Formation of Stable Structures in Microchannels at

Room Temperature. *Adv. Funct. Mater.*, vol. 18, article 1097, 2008.

[49] H. Wang, S. Chen, B. Yuan, J. Liu and X. Sun, Liquid Metal Transformable Machines. *Accounts of Materials Research*, vol. 2, pp. 1227-1238, 2021.

[50] Z. Li, J. Xu, Z. Wu, B. Guo and Q. He, Liquid Metal Swimming Nanorobots. *Accounts of Materials Research*, vol. 3, pp. 122-132, 2022.

[51] X. Sun, B. Yuan, H. Wang, L. Fan, M. Duan, X. Wang, R. Guo and J. Liu, Nano-Biomedicine based on Liquid Metal Particles and Allied Materials. *Adv. NanoBiomed Res.*, vol. 1, article 2000086, 2021.

[52] S. Chen and J. Liu, Pervasive liquid metal printed electronics: From concept incubation to industry. *iScience*, vol. 24, article 102026, 2021.

[53] H. Liu, M. Li, Y. Li, H. Yang, A. Li, T. Lu, F. Li and F. Xu, Magnetic steering of liquid metal mobiles. *Soft Matter*, vol. 14, 3236-3245, 2018.

[54] L. Hu, H. Wang, X. Wang, X. Liu, J. Guo and J. Liu, Magnetic Liquid Metals Manipulated in the Three-Dimensional Free Space. *ACS Appl. Mater. Interfaces*, vol. 11, pp. 8685-8692, 2019.

[55] H. Wang, S. Chen, H. Li, X. Chen, J. Cheng, Y. Shao, C. Zhang, J. Zhang, L. Fan, H. Chang, R. Guo, X. Wang, N. Li, L. Hu, Y. Wei and J. Liu, A Liquid Gripper Based on Phase Transitional Metallic Ferrofluid. *Adv. Funct. Mater.*, vol. 31, article 2100274, 2021.

[56] S. Handschuh-Wang, L. Zhu, T. Gan, T. Wang, B. Wang and X. Zhou, Interfacing of surfaces with gallium-based liquid metals – approaches for mitigation and augmentation of liquid metal adhesion on surfaces. *Appl. Mater. Today*, vol. 21, article 100868, 2020.

[57] D. Castelvechi, New Instrument for Solo Performance. *Phys. Rev. Focus*, vol. 15, pp. 18, 2005.

[58] J. Ma, V. T. Bharambe, K. A. Persson, A. L. Bachmann, I. D. Joshipura, J. Kim, K. H. Oh, J. F. Patrick, J. J. Adams and M. D. Dickey, Metallophobic Coatings to Enable Shape Reconfigurable Liquid Metal Inside 3D Printed Plastics. *ACS Appl. Mater. Interfaces*, vol. 13, pp. 12709-12718, 2021.

[59] I. D. Joshipura, H. R. Ayers, G. A. Castillo, C. Ladd, C. E. Tabor, J. J. Adams and M. D. Dickey, Patterning and Reversible Actuation of Liquid Gallium Alloys by Preventing Adhesion on Rough Surfaces. *ACS Appl. Mater. Interfaces*, vol. 10, pp. 44686-44695, 2018.

[60] S. Handschuh-Wang, F. J. Stadler and X. Zhou, Critical Review on the Physical Properties of Gallium-Based Liquid Metals and Selected Pathways for Their Alteration. *J. Phys. Chem. C*, vol. 125, pp. 20113-20142, 2021.

[61] R. Guo, X. Sun, B. Yuan, H. Wang and J. Liu, Magnetic Liquid Metal (Fe-EGaIn) Based Multifunctional Electronics for Remote Self-Healing Materials, Degradable Electronics, and Thermal Transfer Printing. *Adv. Sci.*, vol. 6, article 1901478, 2019.

[62] E. J. Markvicka, M. D. Bartlett, X. Huang and C. Majid, An autonomously electrically self-healing liquid metal-elastomer composite for robust soft-matter robotics and electronics. *Nat. Mater.*, vol. 17, pp. 618-624, 2018.

[63] X. Wang, R. Guo and J. Liu, Liquid Metal Based Soft Robotics: Materials, Designs, and Applications. *Adv. Mater. Technol.*, vol. 4, article 1800549, 2019.

[64] A. Adamatzky, A. Chiolerio and K. Szaciłowski, Liquid metal droplet solves maze. *Soft Matter*, vol. 16, pp. 1455-1462, 2020.